Geologica Acta, Vol.5, Nº 3, 2007, 231-244
Available online at www.geologica-acta.com

geologica acta

3D modelling of grain size distribution in Quaternary deltaic deposits (Llobregat Delta, NE Spain)

P. CABELLO * J.L. CUEVAS and E. RAMOS

Departament d'Estratigrafia, Paleontologia i Geociències Marines.
Geomodels-Group of Geodynamics and Basin Analysis. Facultat de Geologia, Universitat de Barcelona.
Zona Universitària de Pedralbes, 08028 Barcelona

*Corresponding author: E-mail address: pcabello@ub.edu (P. Cabello)

ABSTRACT

The Llobregat delta constitutes a Pliocene-Quaternary sequence recording progradation. An 8 meter-thick, delta-plain succession temporarily accessible in the subaerial delta plain was sub-divided into four units (A to D), which constitute a shallowing upwards sequence recording sedimentation from shoreface at the bottom (Unit A) to lacustrine settings at the top (Unit D). Unit B basically comprises gravelly, coarse-grained sandy lenticular bodies (up to 20 m wide, up to a few decimetres thick), within a homogenous, medium-grained sandy background, interpreted as prograding foreshore bars. 3D facies models, built by using the sequential conditional indicator simulation method, reproduced the sedimentary heterogeneities identified in Unit B, using as input data the sedimentary body geometry and its correlation with sandstone grain size values, with the grain size modes taken as a continuous, quantitative proxy for facies distribution. The simulations not only reproduced satisfactorily the significant sedimentary heterogeneities generated by the facies arrangement, but also predicted and described the spatial relation and the three-dimensional shape of sedimentary bodies accurately. Quality of the models should be ensured by a consistent prior analysis of the spatial structure of the grain size mode based on semivariogram models.

KEYWORDS | **Llobregat delta. Physical properties. Facies modelling. Sequential conditional indicator simulation.**

INTRODUCTION

Characterization of deltas is widely carried out because of their economic and social interest. Determination of permeable/impermeable facies distribution and modelling fluid circulation using geostatistical methods is a common aim in hydrogeology (Huggenberger and Aigner, 1999; Bitzer, 2004; Gonçalvès et al., 2004; Saaltink et al., 2004; Yaramanci, 2004; Zabalza-Mezghani et al., 2004; Lafuerza et al., 2005; Zappa et al., 2006; Falivene et al., 2007a, 2007b; Falivene et al., in press) and in hydrocarbon reservoirs (MacDonald et al., 1992; Jian et al., 2002; Castellini et al., 2003; Larue and Legarre, 2004; Svanes et al., 2004; Ainsworth, 2005; Falivene et al., 2007a). Geostatistical analysis simulating aquifer facies distribution should be developed with a solid knowledge of sedimentary body architecture, and considering sedimentary heterogeneities affecting flow predictions (Dreyer et al., 1993;

Deutsch, 1999). Geological data about the geometry, arrangement and petrophysical characteristics of sedimentary bodies are useful tools for improving 3D subsurface facies modelling, because they reduce uncertainties associated with predicting interwell areas (Dreyer et al., 1993; Li and White, 2003; Larue, 2004; Satur et al., 2005; Cabello et al., 2006; Falivene et al., 2006a, 2006b).

Heterogeneities identified in the sedimentary record and associated with sedimentary bodies, such as subaerial or subaquatic channels, mouth bars in a deltaic environment or shoreface bars, are recognized by facies changes (lithology, sedimentary structures, palaeobiological remains, etc.), as well as by the geometry and arrangement of these bodies. Physical properties of sediments are often conditioned by the sedimentary processes that originated the deposits (because of this, facies usually correlate with physical parameters in clastic reservoirs or aquifers); and, in turn, physical properties determine flow performance through the sedimentary formation.

This paper focuses on the incorporation of sedimentary heterogeneities as a fundamental premise for geostatistical studies of aquifer modelling. Its aim is to verify the efficiency of the sequential conditional indicator simulation method in generating models of anisotropic sedimentary bodies arranged on a homogeneous background. The sequential indicator algorithm has been tested before in both aquifer and reservoir modelling (de Marsily et al., 1998; Deutsch, 1999; Falivene et al., 2006a). The present paper contributes to Llobregat delta characterization by providing information on deltaic sediments and testing the efficiency of a geostatistical application in reproducing sedimentary bodies that are several decimetres thick and some meters wide, with the aim of building an accurate and consistent aquifer model.

GEOLOGICAL SETTING

The Llobregat River is located in NE Spain. It springs from the Pyrenees range and flows to the Mediterranean Sea. At its mouth, this river forms a 97 km^2 moderate-sized wave-dominated delta (Fig. 1A).

Previous studies defined the Llobregat delta as a lobate type whose present-day shape is controlled by the equilibrium between fluvial sediment input and littoral

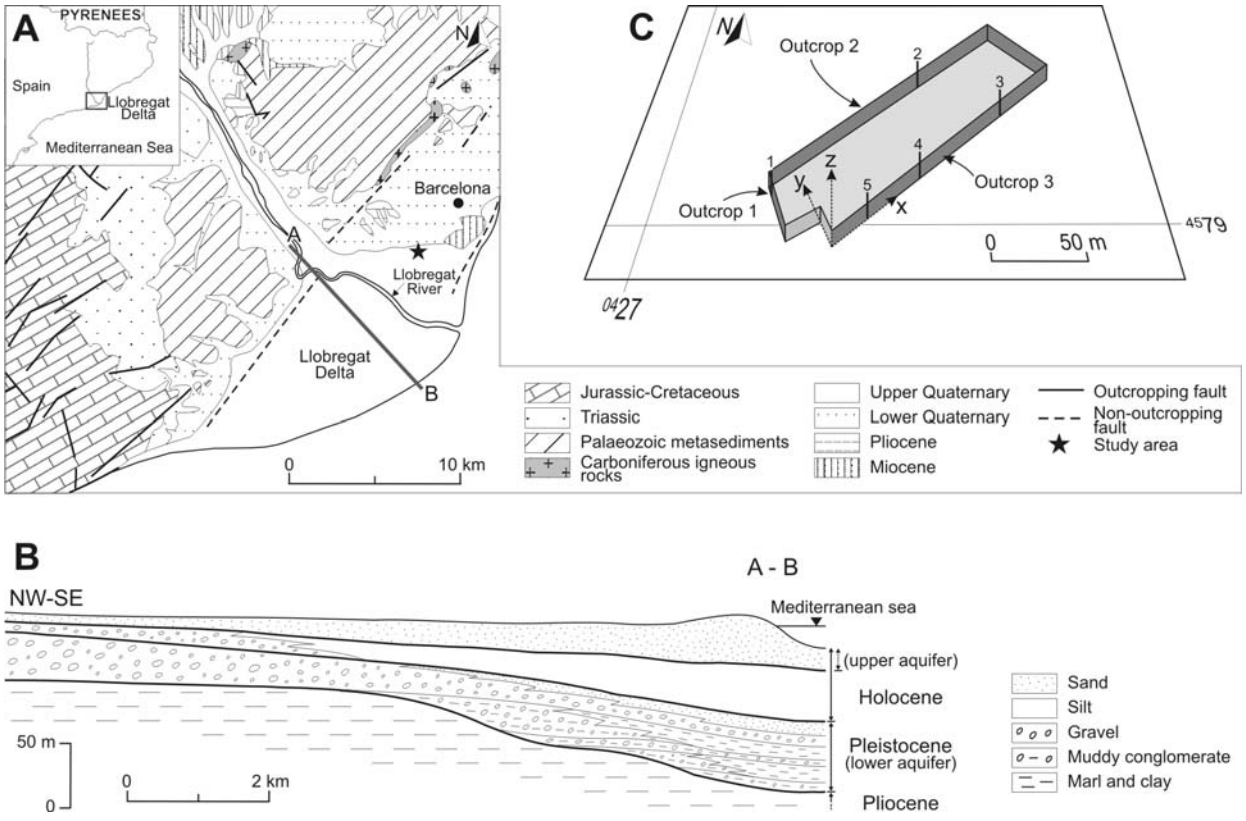

FIGURE 1 | **A) Location and geological sketch of the Llobregat delta and its surroundings. Modified from Marqués (1974). Cross-section A-B is shown in B. See star in A for location of the studied area in C. B) NW-SE cross-section of the Llobregat delta. Modified from Manzano et al. (1986-1987). See location (A-B) in A. C) Sketch of the studied zone and orientation of the outcrops. Numbers 1 to 5 correspond to location of sedimentological logs shown in Figure 4. Coordinates are in kilometres in Universal Transverse Mercator (UTM) zone 31.**

modelling by swell and longshore currents (Marqués, 1974, 1984; Manzano, 1986; Manzano et al., 1986-87). The delta is formed by a sedimentary package ranging from Pliocene to Quaternary in age, even though its present-day size is the result of delta progradation during the last Holocene post-glacial marine highstand (Manzano et al., 1986-87). The delta body is split into four non-formal units (Marqués, 1984; Manzano et al., 1986-87), which are from base to top (Fig. 1B): 1) a lower unit, consisting of blue marls and clays containing marine Pliocene fauna; 2) Pleistocene muddy conglomerates that pass basinwards to marls and clays, and are overlain by a coarser sequence of gravels interfingered basinwards with sands; 3) Holocene marine silts interfingered landwards with proximal gravels; and 4) the recent upper unit, mainly formed by clean, well-sorted sands. Both the Pleistocene and the Recent upper sandy delta units constitute two aquifers, named the lower and the upper aquifers, respectively.

This study focuses on a sector (140 m long, 40 m wide, Fig. 1C) of the Llobregat delta plain, corresponding to the trenches excavated on a building site. The uppermost 8 meters of the delta plain belong to the upper unit cropped out as a result of this excavation. The sedimentary record mainly corresponds to clean sands, with minor gravels and shallow lacustrine-marsh mudstone and peat.

METHODOLOGY

The study was developed in four basic steps (Fig. 2): 1) definition of sedimentary body geometry by using photomosaics and drawings of outcrops (Fig. 3). Three different photomontages were obtained from three trench outcrops, which were oriented in two nearly perpendicular directions (see Fig. 1C); 2) sedimentological and stratigraphic characterization, and facies analysis of the sedimentary record, supported by 5 logs (Fig. 4) and the above study of sedimentary body geometry; 3) sampling and measurement of physical properties (grain size, permeability and porosity) of unaltered sediment samples (Table 1), and analysis of the correlation between sedimentary bodies and physical properties (Table 2, Figs. 3 and 5), on which the geostatistical analysis (the last methodological step) is based. Grain size analyses were made by using a *Coulter LS 100* system. Permeability tests were performed in a variable level permeameter, and bulk porosity was obtained by the water immersion method; and 4) exploratory statistical analysis of physical data (grain size, permeability and porosity) and geostatistical simulation of facies distribution, by the sequential conditional indicator method (Figs.7 and 8).

STRATIGRAPHY, SEDIMENTOLOGY AND GEOMETRY OF THE SEDIMENTARY BODIES

On the basis of their grain size, sedimentary structures and palaeobiological content, seven sedimentary facies (facies 1 to 7) were distinguished. Their main characteristics are summarized in Table 2. These seven individual facies can be grouped in four units (A to D; Figs. 3 and 4), in which the sedimentary record was subdivided. These units constitute nearly tabular, continuous bodies, whose boundaries are slightly irregular.

Unit A

This unit is at least 3 m thick, though its lower boundary was not established (Figs. 3 and 4). It is mainly composed of facies 1, with subordinate amounts of facies 3. They are fine-grained sands locally grading upwards to medium or coarse sands, forming coarsening-upwards sequence (logs 3 and 5 in Fig. 4). Sand and gravel form lenses that are a few decimetres long and a few centimetres thick, and are interbedded with pebble horizons. Small-scale wave ripples are widespread, while current ripples and parallel lamination are scarce. Bioturbation is intense, mainly in the lower part. The unit's fossil content is characterized by scarce vegetal remains and abundance of bivalves, especially in its upper part. Remains of *Mactra stultorum* (*L.*, 1758), *Glycimeris bimaculata* (POLI, 1795),

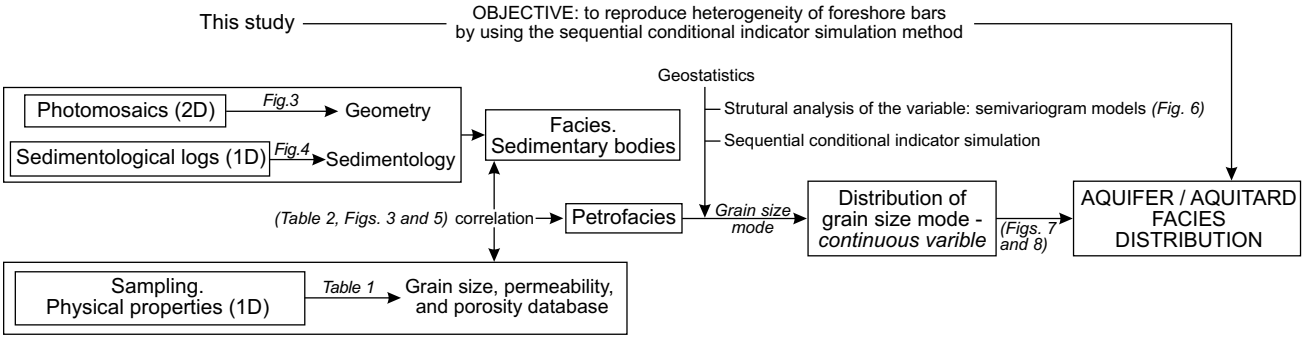

FIGURE 2 | **Methodological flow chart for this study.**

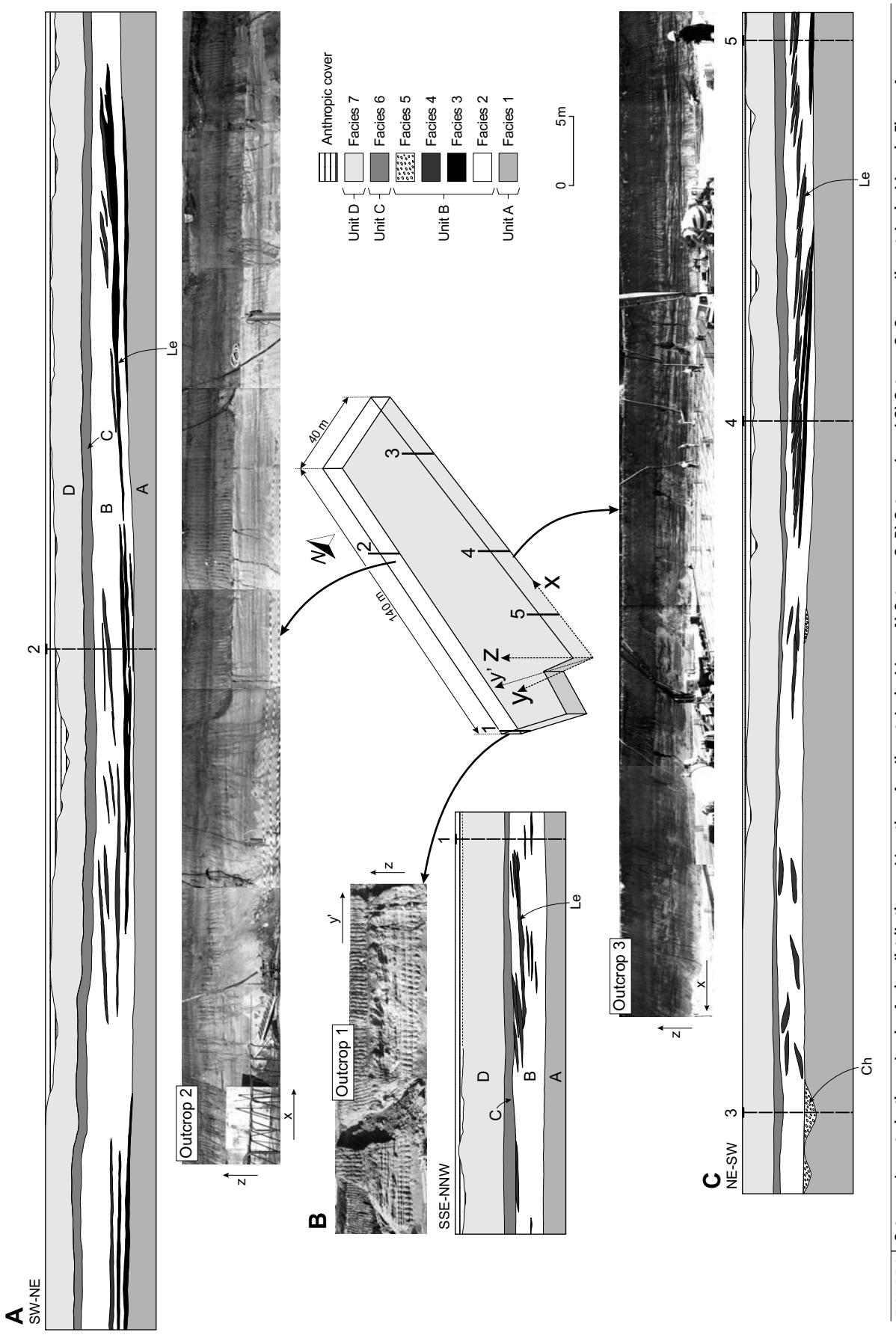

FIGURE 3 | **Outcrop characterizations showing facies distribution and location of sedimentological logs. A) Outcrop 2; B) Outcrop 1, and C) Outcrop 3. See sedimentological logs in Figure 4.**

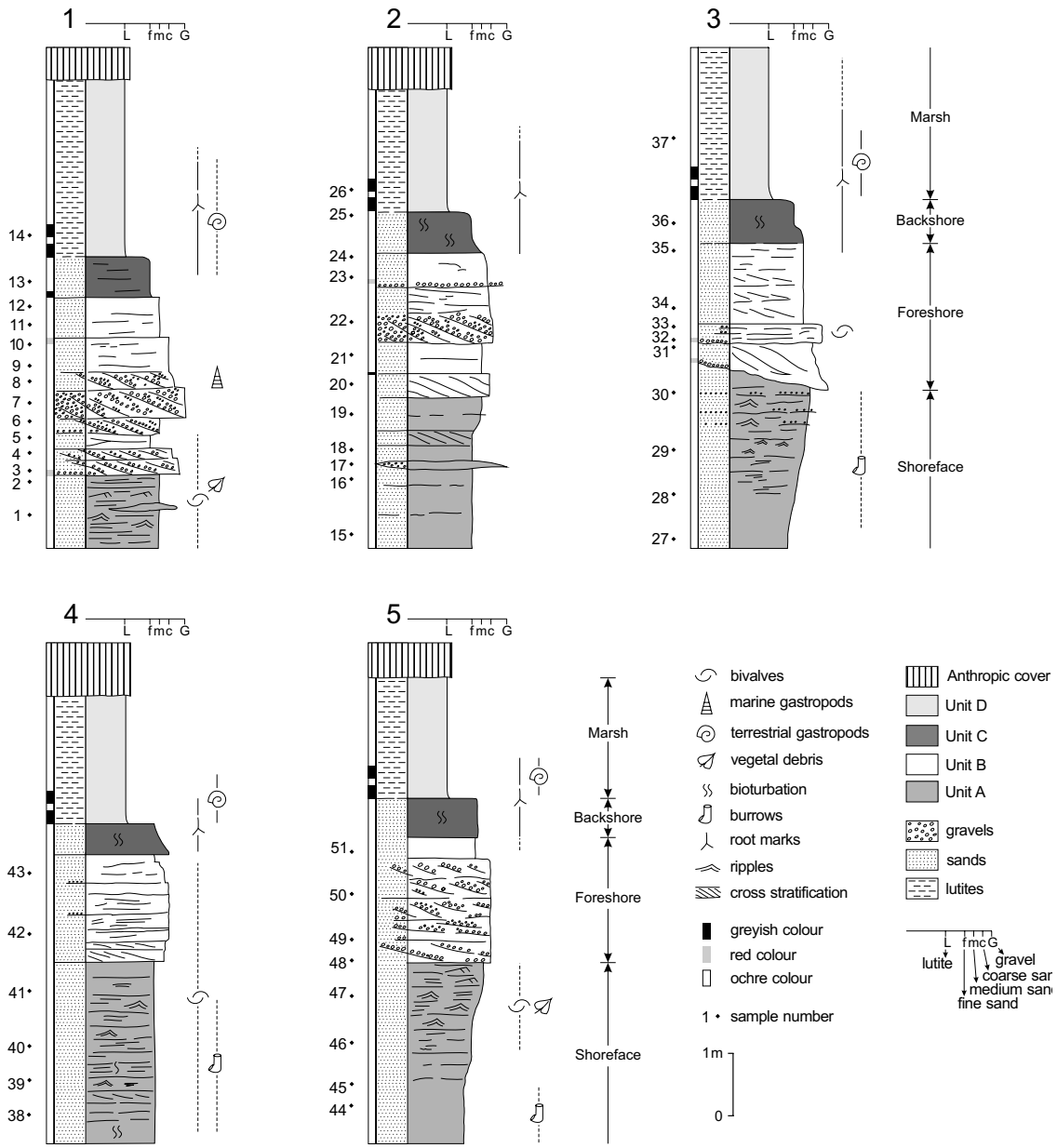

FIGURE 4 | **Sedimentological logs (see location in Figs. 1C and 3). A to D are the depositional units described in the text. Numbers 1 to 5 show the position of the studied samples (physical values in Table 1).**

Donax trunculus (*L.*, 1758) and *Tellina planata* (*L.*, 1758) were identified.

Unit B

This unit varies in thickness from 1.75 to 3.5 m (Figs. 3 and 4). It consists of well-sorted medium and coarse-grained sands and gravels, with cross lamination and planar cross-bedding (Fig. 4), which can be attributed to facies 2, 3, 4 and 5. The gravels frequently display scoured bases and form two different kinds of bodies: groove (Ch in Fig. 3C) and lenticular bodies (Le in Fig. 3). The former are approximately 3 m wide and 50 cm thick. Lenticular bodies have greater horizontal continuity, reaching lengths of up to 20 m, although they are only a few decimetres thick (Fig. 3). These lenticular bodies dip gently to S-SE. Unit B is characterised by a scarce fossiliferous content consisting of gastropods and bivalves (*Chlamys varia* [*L.*, 1758]).

The geostatistical simulation reported in this study was applied to this unit.

TABLE 1 | **Physical values of the samples and facies correspondence studied.**

Log	S	Grain size (μm) Mode		K (m/day)	Φ (%)	Facies
1	1	137.9				1
	2	153.5		3.6	53.7	1
	3	380.0	2739			3
	4	325.0	2739			3
	5	235.7		17.1	25.3	2
	6	292.0	2739			3
	7	325.0	2739			3
	8	390.0	1789			4
	9	390.0	1789	23.6	32.6	4
	10	262.3	1414	28.6	29..8	4
	11	262.3	1414			4
	12	325.0	1100			2
	13	292.0	1100	17.6	35.4	6
	14	8.5				7
2	15	153.5				1
	16	190.2		12.0	39.9	1
	17	292.0	2739			3
	18	262.3		9.2	41.7	1
	19	211.7				1
	20	211.7	2449			3
	21	262.3	1414	14.7	40.9	2
	22	262.3	1789	20.3	36.3	4
	23	211.7	1789	16.1	36.9	4
	24	262.3	1414			4
	25	262.3	1789	14.9	32.9	6
	26	8.5				7
3	27	153.5		2.9	42.3	1
	28	89.8		0.7	40.5	1
	29	100.0		1.7	40.3	1
	30	170.8		7.5	45.7	1
	31	350.0	1265	20.7	33.3	5
	32	211.7	2236	30.7	29.5	5
	33	400	2236	29.8	15.7	5
	34	211.7		15.1	32.1	2
	35	448.4	1265	31.8	42.1	2
	36	262.3		0.9	33.3	6
	37			0.1		7
4	38			9.3	41.6	1
	39			8.3	39.1	1
	40	153.5		6.2	45.7	1
	41			7.8	43.0	1
	42			18.5	34.3	4
	43			24.3	33.8	4
5	44	211.7		4.9	42.6	1
	45	137.9		2.7	47.1	1
	46	170.8		2.6	42.3	1
	47	190.2	2700	8.2	41.5	1
	48	211.7	2700	10.0	38.7	1
	49	263.2	2739			3
	50	263.2	1265	11.9	34.4	4
	51	211.7	1265	6.9	40.8	2

S is sample identification; K is permeability in m/day; ϕ is porosity in %. Grain size in μm. See sample location in Figure 4.

Unit C

Unit C consists exclusively of facies 6, a single, massive, fining-upwards layer ranging from 0.50 to 0.75 m in thickness (Figs. 3 and 4). It is composed of medium- to fine-grained arkoses to subarkoses. Its massive appearance is related to pervasive root bioturbation, indicated by root marks. Its palaeontological remains content is negligible.

Unit D

This unit is 2 to 2.5 m thick (Figs. 3 and 4). It is exclusively made up of facies 7, consisting of brown-grey massive lutites. Towards the bottom of the unit, two dark-grey peaty beds about 15 cm thick occur. Root marks and vegetal remains are frequent, as well as terrestrial gastropod shells of *Helix aspersa* (MÜLLER, 1774) and *Cochlicella barbara* (*L.*, 1758).

Interpretation

The fine- to medium-grained sands showing tractive sedimentary structures and diverse degree of bioturbation (mainly facies 1), which characterize Unit A, are interpreted as shoreface deposits generated under wave action on the delta front (Bhattacharya and Walker, 1992; Reading and Collinson, 1996). The gravels and coarse-grained sandy horizons indicate higher environmental energy episodes, whereas the presence of terrestrial vegetal remains records contributions from the continent and suggests the proximity of palaeoshore and subaerial emerged zones.

The coarser-grained sands (facies 2, 3, 4 and 5) constituting Unit B indicate an increase in environmental energy, probably related to a shallowing trend. The arrangement and geometry of the lenticular bodies of cross-bedded gravels and coarse-grained sands (Le in Fig. 3) correspond to small-scale foreshore bars (Ricci Lucchi, 1978; Reading and Collinson, 1996) prograding towards the SE, in a direction perpendicular to the shoreline. The groove bodies (Ch in Fig. 3C) could be interpreted as transversal-like sections of small channels arising from the closer continent.

Although the palaeontological remains content of Unit C is negligible, the high root bioturbation and the fining-upwards trend of the sediments could indicate that Unit C is the result of sedimentation in a backshore zone, where low energy settings are frequent (Bhattacharya and Walker, 1992; Reading and Collinson, 1996).

The ochre, greyish, fine-grained detrital sediments, with abundance of root traces and gastropods of terrestrial origin, which characterize Unit D, suggest deposition in a

TABLE 2 | **Physical, sedimentological and geometrical characteristics of the facies defined (1 to 7).**

Facies	Lithology	Grain size (μm)	K (m/day)	Φ (%)	Geometry	Palaeoenvironment	Unit
1	fine to medium sand	n=16 unimodal R= 89.8 - 262.3	n=16 R= 0.7 - 12.0	n=16 R= 38.7 -53.7	lower boundary not recognized	shoreface	A
2	medium sand	n=6 bimodal R= 211.7 - 448.4	n=5 R= 6.9 - 31.8	n=5 R= 25.3 - 42.1	tabular	foreshore	B
3	gravel and coarse sand	n=2 bimodal R= 2449 - 2739	-	-	lenticular	foreshore	B(A)
4	coarse and medium sand	n=8 bimodal R= 1265 - 1789	n=5 R= 11.9 - 28.6	n=5 R= 29.8 - 36.9	lenticular	foreshore	B
5	gravel and coarse sand	n=3 bimodal R=1265 - 2236	n=3 R= 20.7 - 30.7	n=3 R= 33.3 - 15.7	groove	foreshore	B
6	medium to fine-grained arkoses	n=3 bimodal (unimodal) R= 262.3 - 292.0	n=3 R= 0.9 - 17.6	n=3 R= 32.9 - 35.4	tabular	backshore	C
7	lutites	n=2 unimodal R= 8.5	n=1 R= 0.1	-	tabular	marsh	D

n is the number of samples for each facies; R is the range values of grain size (in μm), permeability (K, in m/day) and porosity (ϕ, in %) observed from sample values of Table 1.

calm, underwater environment, possibly in a pond or marsh zone, in the vicinity of the backshore (Ricci Lucchi, 1978; Arche, 1992) in the lower delta plain. The two black, peaty beds identified on the lower part of the unit would indicate episodes of higher plant contribution at the bottom of the pond.

In conclusion, the sequential arrangement of the sedimentary record corresponds to a shallowing upwards sequence in a transitional coastal environment, recording sedimentation from the marine shoreface to a marsh, from a delta front to a lower delta plain (Arche, 1992; Bhattacharya and Walker, 1992; Reading and Collinson, 1996). This sequence records the last episode of the Holocene progradation of the Llobregat delta (Gámez et al., 2005).

GEOSTATISTICAL ANALYSIS

Robust 3D facies models of hydrocarbon reservoirs or aquifers should capture sedimentary heterogeneities relevant to flow (Dreyer et al., 1993; Deutsch, 1999). Sedimentary heterogeneities control the anisotropy and variability of physical properties of deposits through space. Facies and physical properties are closely related. The seven above-mentioned facies types were described on the basis of the correlation between sedimentology, geometry and physical properties (Table 2 and Figs. 3, 4 and 5). These facies types constitute sedimentary bodies characterized by a defined geometry (Fig. 3) and a range of physical values (Table 1), and resulted from sedimentation in specific environmental settings (Fig. 4). For instance, facies 4, which was deposited in a foreshore environment (Unit B), comprises lenticular bodies of coarse- and medium-grained sand with bimodal distribution of grain size, permeability values from 11.9 to 28.6 m/day and porosity values ranging from 29.8 to 36.9%.

The facies classification (Table 2) is mainly based on distribution of grain-size populations (bi or unimodal) and modal values (grain size). Samples with bimodal grain-size distribution are considered matrix-rich, with the larger size mode corresponding to the size of the grains and the smaller size representing the matrix. Permeability or porosity properties display poorer correlation with facies and sedimentary bodies than grain size (Figs. 5A, B and C). This low correlation has two possible causes: 1) the range of permeability and porosity values for each facies types frequently overlap, and 2) the small number of samples tested for permeability or porosity compared with samples analysed for grain size measurements (Table 1 and Figs. 5A, B and C). Thus, the close relationship between grain size and the respective facies allowed us to build models based on the distribution of a quantitative and continuous variable instead of a qualitative and categorical variable, like facies. The grain size model results can become the input for subsequent physical parameter distribution suitable for flow simulation.

To sum up, this study assumed that the grain size mode is directly related to the facies, and so can be considered a proxy for facies distribution (Fig. 2). Taking into account the facies geometry described above and based on photomosaic interpretation (Table 2 and Fig. 3), we

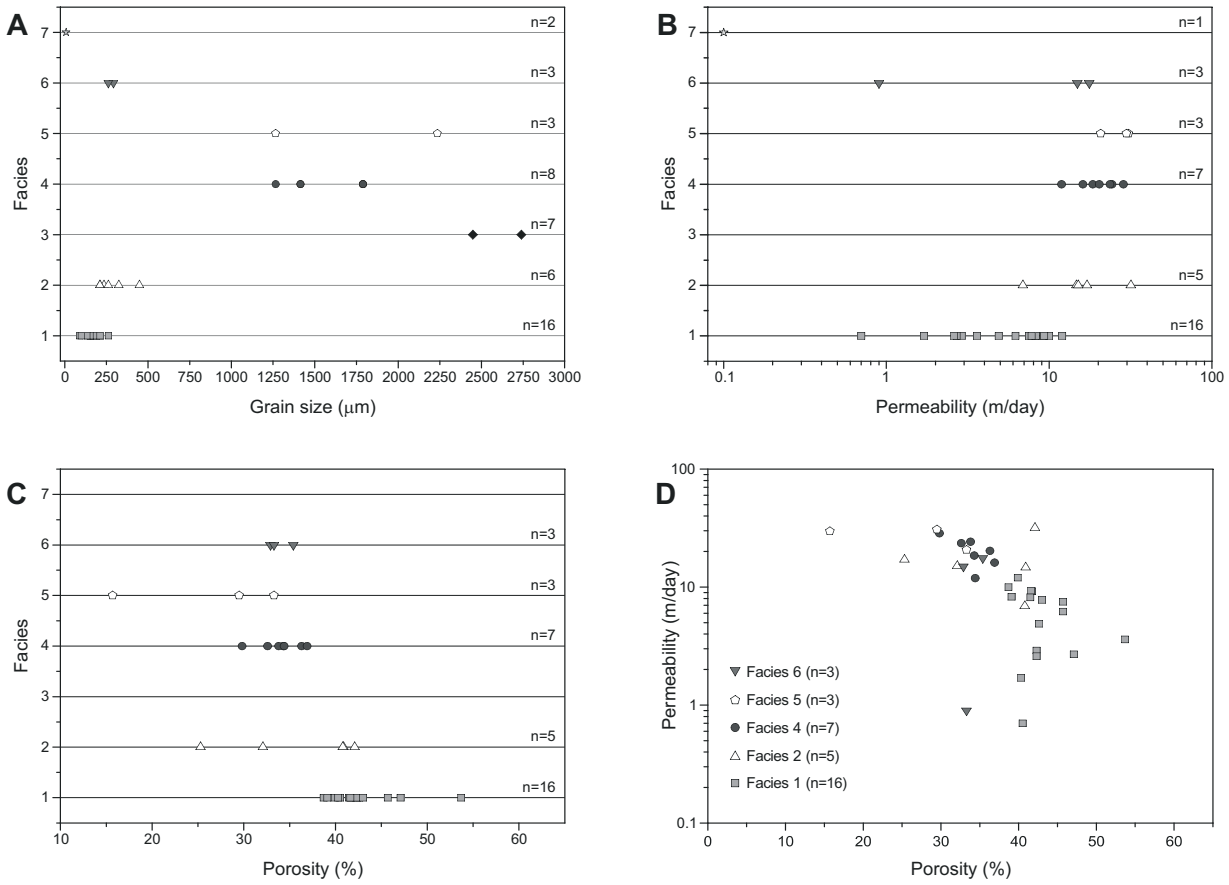

FIGURE 5 | **Grain size (A), permeability (B) and porosity (C) values *versus* facies. (D) Permeability *versus* porosity. Note that data dispersion for grain size values *versus* facies is lower than for porosity and permeability *versus* facies, which indicates higher correlation between grain size and facies than between permeability or porosity and facies. n is the number of samples for each facies type.**

considered that the sedimentary heterogeneities produced by the lenticular bodies (facies 3 and 4) inside the four units have significant implications in flow simulations, because these facies have different physical characteristics from the background sediments (Tables 1 and 2, Fig. 5) and their geometry and arrangement add sedimentary anisotropy to the aquifer (Fig. 3). Facies 4 shows high, very homogenous permeability-porosity relations (Fig. 5D), which indicates low variability of physical properties along this facies type if compared to the background (facies 2, Fig. 5). Although no permeability or porosity values sampled facies 3, similar values of facies 4 were inferred for facies 3, by analogy in grain size distribution and body geometry. Consequently, geostatistical methods applied to modelling should properly reproduce these lenticular bodies.

The geostatistical method

Sequential conditional indicator simulation

Grain-size distribution models were obtained by the sequential conditional indicator simulation method. Simulation is the process of building alternative equally probable realizations based on the spatial distribution of the variable (Deutsch and Journel, 1992). Simulation provides many alternative numerical models, each of which is a "good" representation of reality in some general sense. The differences between these alternative models or realizations provide a measurement of joint spatial uncertainty (Deutsch and Journel, 1992).

Sequential conditional indicator simulation is a cell-based algorithm (Deutsch, 1999; Falivene et al., 2006a, 2007a). This statistical technique involves the application of the general sequential simulation method to the case of an indicator function, or more generally of several nested indicators (Chilès and Delfiner, 1999). The indicator function transforms the variable into a new property, which is the probability of finding the original value of the related variable at a given position (Journel and Alabert, 1989; Gómez-Hernández and Srivastava, 1990; Falivene et al., 2006a, 2007a). The indicator value is one at a grid cell position if the considered value of the variable exists (or is estimated) at that location; if not, the indicator is set to

zero. The sequential simulation principle is a generalization of this idea: the conditioning (honouring data at certain locations) is extended to include all data available in the neighbourhood of a given point, including the original data and all previously simulated values (Deutsch and Journel, 1992).

The sequential conditional indicator method is suitable for simulations of both categorical variables (i.e. facies) and continuous variables (i.e. grain size values). As grain size is a continuous variable, by applying the sequential conditional indicator simulation method the

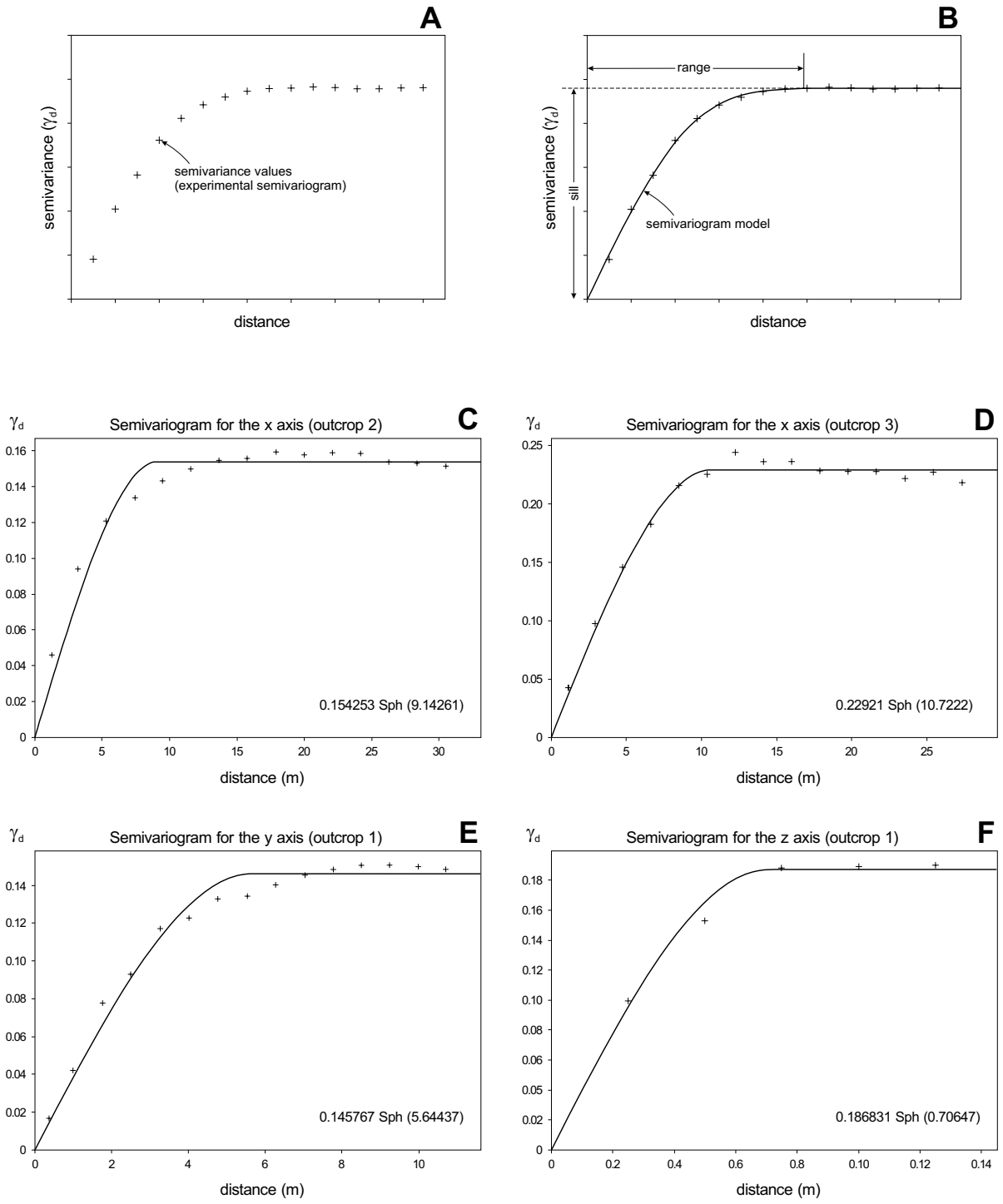

FIGURE 6 | **Sketches of an experimental semivariogram (A) and a semivariogram model (B) based on A. Semivariogram models showing the continuity of the grain size mode along the x, y and z axes: x axis for outcrop 2 (C) and for outcrop 3 (D), y axis for outcrop 1 (E) and z axis for the outcrop 1 (F). Outcrop interpretation is shown in Figure 3.**

value given to a cell is one if the estimated value of grain size mode at that point is above, or below, a certain threshold. Otherwise, the cell value is zero.

The geostatistical process and semivariograms

Even though grain size mode is spatially continuous, its value at every point cannot be known. Instead, its values are known only through samples situated at specific locations (Davis, 1986). The variable is related and characterised by properties of these samples, on which its spatial distribution is also based. Changes of sample values also involve changes in variable and spatial structure. In the present study, these samples not only comprise the 45 physical values of Table 1, but photomosaic interpretation also informs on the size and orientation of sedimentary bodies (facies, Fig. 3), which match up with certain grain size values. For each facies type, unsampled sedimentary bodies were given grain size values of the most frequent grain size modes of Table 1. As the sedimentary heterogeneity under consideration only occurs in Unit B, models were constructed only for this unit.

Semivariance is a measurement of the degree of spatial dependence between samples along a specific support (Davis, 1986). We calculated semivariances for values of grain size mode and projected them onto an experimental semivariogram (Fig. 6A). To calculate predictions and/or simulations of grain size, an analytical model must be fitted to the experimental semivariogram: the semivariogram model (Fig. 6B), which describes the spatial structure of grain size. Since models reproduce the grain size heterogeneity of lenticular bodies, the experimental semivariograms obtained (Figs. 6C, D, E and F) describe the continuity of the variable at values above 700 μm, a representative grain size for lenticular bodies of facies 3 and 4 (Tables 1 and 2, Fig. 5A).

The photomosaic interpretation of Fig. 3 was used to establish the degree of spatial dependence of grain size.

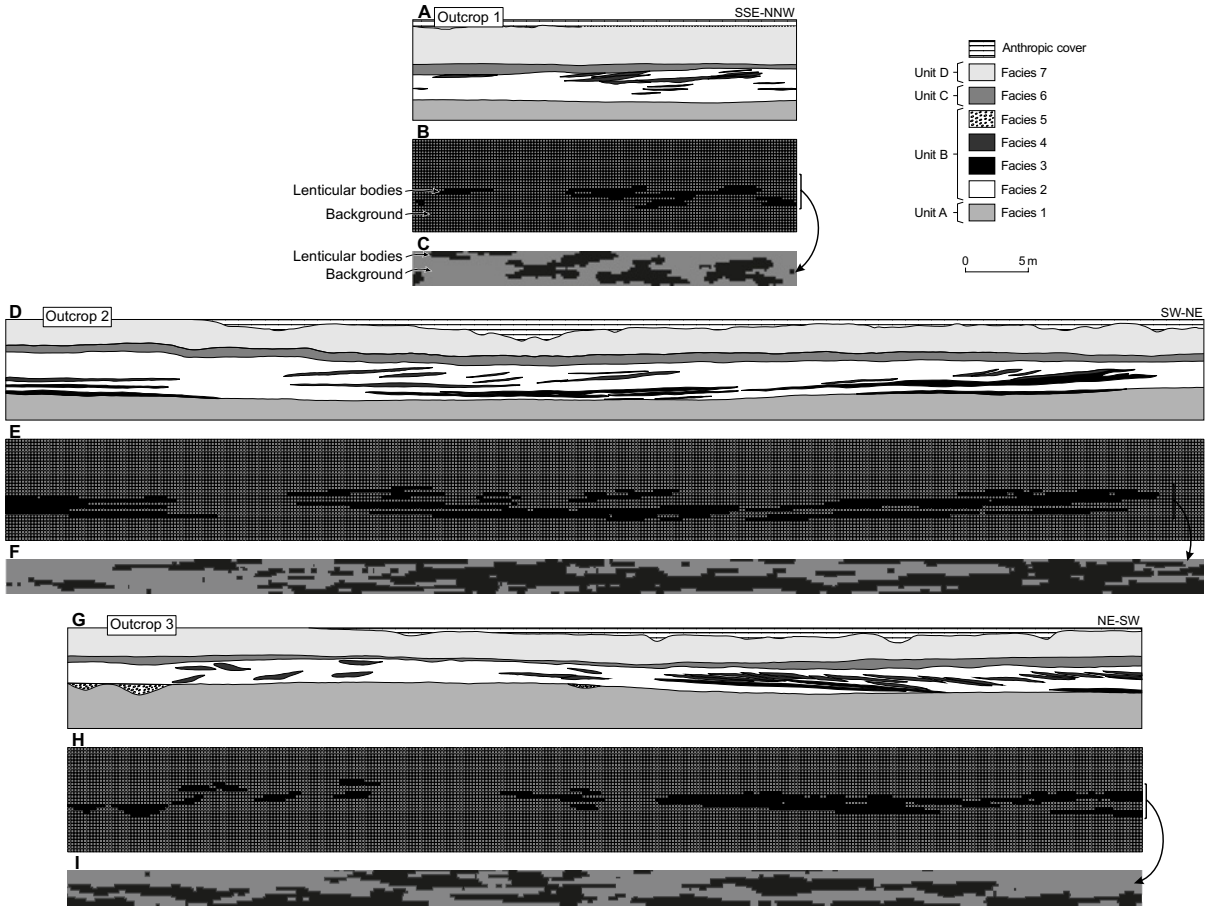

FIGURE 7 | **Outcrop discretization (B, E and H), 25 cm-resolution, based on previous interpretation of facies distribution (A, D and G). Visual results of sequential conditional indicator simulations for each outcrop (C, F and I) are shown. Black cells indicate values of grain-size mode coarser than 700 μm and represent facies of gravelly, coarse- and medium-grained sandy lenticular foreshore bars. Grey cells indicate grain size modes finer than 700 μm representing the background.**

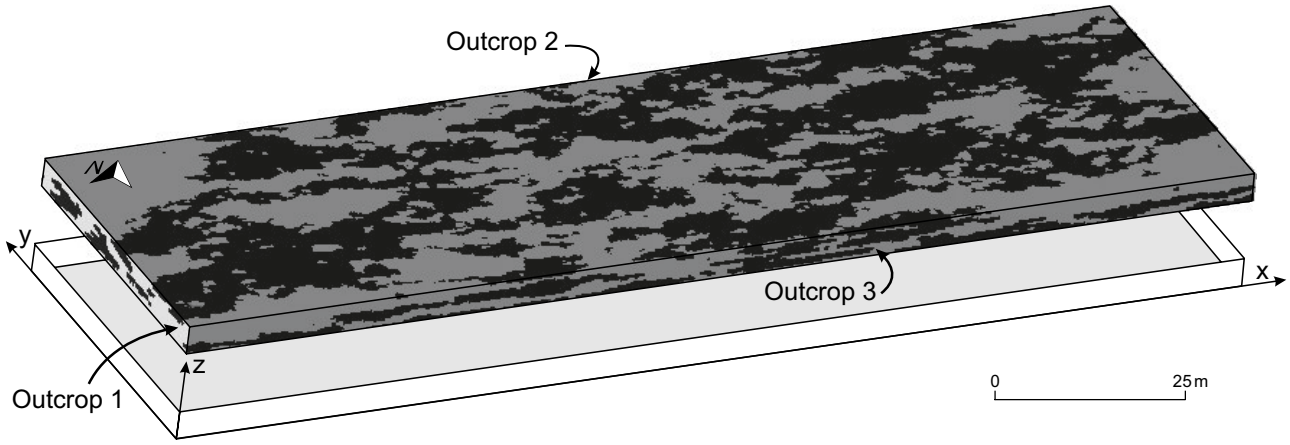

FIGURE 8 | **Visual results of models showing grain size distribution resulting from the application of the sequential indicator simulation method to the sedimentary record of Unit B. Dark zones indicate grain size modes coarser than 700 μm, while in greyish sectors the grain size is finer than 700 μm. Note that dark sectors are lengthened morphologies in vertical sections and oval viewed from the top. These bodies reproduce the gravelly, coarse- to medium-grained sandy lenticular foreshore bars.**

We proceeded by discretizing the three cross-sections into 2D grids of 25 x 25 cm cell size (the grid resolution should respect the minimum size of the body to be reproduced). Each cell, referenced to an x, y, z coordinate system (Fig. 3), was given the appropriate value of grain size mode, taken from the original photomosaic interpretation (Fig. 7). A database of cell position and the corresponding indicator value (zero if the grain size is below 700 μm or one otherwise) of the grain size became the input to three experimental semivariograms, one of them for each axis and coinciding with the outcrop directions, on which, consequently, the semivariogram models are based (Figs. 6C to F).

Semivariograms are structured into different regions: for short distances, the semivariogram resembles a linear function; while, if distance increases, the function adapts to a curve until it reaches a constant semivariance value, the sill (Fig. 6B). This distance, at which the semivariogram develops a flat region, is called range (Fig. 6B), and it defines a neighbourhood within which all locations are related to one another (Davis, 1986) and the values have some degree of spatial continuity. The ranges of the semivariogram models of outcrops 2 and 3 (Figs. 6C and D) are similar (9.14 m and 10.72 m, respectively) and larger than the range of outcrop 1 (5.6 m, Fig. 6E), because the major continuity of grain size values (and consequently, of facies) observed is consistent with the direction of outcrops 2 and 3, i.e. SW-NE (x axis, Fig. 3). Along this direction, lenticular bodies of several metres length were described (Fig. 3). Likewise, the intermediate continuity of grain size coincides with the direction of outcrop 1 (y axis, Fig. 3), which is the NNW-SSE apparent progradation direction of the lenticular bodies (to the SSE). Lenticular body thickness, however, shows the minor continuity of grain size (z axis, Fig. 3).

Semivariograms for the z axis show a pure nugget effect, although a certain spatial correlation along the vertical axis can be qualitatively inferred from the observation of the facies diagrams. Assuming that such a nugget effect is related to the smaller density of sampling along the vertical direction together with strong anisotropy related to stratification, resampling at a finer scale (gridding of the facies diagrams at a 10 x 10 cm grid) and rescaling of the z axis (multiplied by 10) was performed (Fig. 6F). Semivariograms calculated on such transformed diagrams show a higher spatial correlation for outcrop 1 than original non-rescaled semivariograms, although outcrops 2 and 3 maintain an uncorrelated spatial structure. The range of the semivariogram of outcrop 1 after rescaling of the range (the range has been divided by 10, since this is the value for the multiplier of the transformed z axis) was chosen as the valid vertical range for the simulations (Fig. 6F).

The sill of semivariogram models used is non-standardized, since, in sequential indicator simulation method, the spatial structures are not limited by Gaussianity (Gómez-Hernández and Srivastava, 1990). The sill of the semivariogram of outcrop 3 was chosen for simulation because it provides a good approximation to facies proportions in the studied unit (Fig. 6). The semivariogram range for x axis used is the one measured in outcrop 3 (10.72 m), and this range is also a good approximation to the range measured from outcrop 2 (Figs. 6C and D). The range of the semivariogram of outcrop 1 (5.6 m, Fig. 6E) was the range for the y axis. Simulations of grain size field using the sequential conditional indicator method to reproduce the spatial distribution of the lenticular bodies were based on the spatial continuity of grain size described by the semivariogram models. Qualitative,

visual comparisons between the real and simulated outcrops are given in Figs. 7 and 8.

DISCUSSION

The trench excavations in the studied zone provided artificial outcrops located in an urban, highly inhabited area, where outcrops are exceptional. We had available an adequate sedimentological (outcrops and photomosaics) and physical property database (grain size, porosity and permeability). Nevertheless, the expanse of the outcrop (140 m x 40 m x 8 m) is relatively limited if compared with the whole of the delta. As a consequence, the results of this research are mainly methodological, since the objective was to test the efficiency of the sequential conditional indicator simulation method in building models of gravelly, coarse- and medium-grained sandy lenticular bodies in a medium-grained sandy background. Although the sedimentary record comprises other sedimentary units (Units A, B and D) and facies (facies 5, Fig. 3 and Table 2), apart from lenticular bodies and the background of medium sands of Unit B, the method simplified the modelling simulating distribution of facies 3 and 4 for the record of Unit B to provide the most important heterogeneity (Figs. 7 and 8). The spatial distribution of the larger, delta-scale sedimentary bodies needs to be supported by more data (outcrops and/or bore-holes), covering a wider area and thicker stratigraphic record, as in the case of Lafuerza et al. (2005).

The quality of the simulations depends on the quality of the structural analysis of the variable performed (Gringarten and Deustch, 2001), i.e. defining at what point the semivariogram models conform to the actual spatial structure of the variable. This is also largely a matter of how the variable was sampled. Conditional simulations honour the observed values at some given locations, which in this study are the data from sedimentological logs. The more locations are available as conditioning values, the lower will be the variability between different conditional realizations (Journel and Alabert, 1989). In the limit, provided there are enough conditioning values, the outcome from conditional simulations will not differ substantially from an interpolation between these values.

Three-dimensional appropriate models improve knowledge of aquifer or reservoir structure by predicting and explaining the geometry of lenticular bodies in 3D, generating new, complete and precise images about the 3D geometry of these sedimentary bodies and the spatial relationship between them.

Visual results of modelling (Figs. 7 and 8) show certain dark-coloured sectors, which correspond to zones where the indicator is one (i.e. the grain size mode is coarser than 700 μm), alternating with greyish sectors where the indicator is zero (the grain size is finer than 700 μm). The close correspondence and coincidence between the original outcrop interpretations and equivalent sections of models (Fig. 7) reveal that the models built using the sequential conditional indicator method satisfactorily reproduce foreshore bar heterogeneities.

As Fig. 8 illustrates, certain sectors of the models, recording grain-size values coarser than 700 μm (dark colour), have long, thin shapes in vertical sections and become oval viewed from the top, floating on a background whose grain size mode is below 700 μm. These bodies with high-grain size values (which could be related to bodies with high-to-moderate permeability and porosity) are partially disconnected in vertical direction but have high horizontal continuity, and reproduce the gravelly, coarse- to medium-grained sandy lenticular foreshore bars. In addition, these bars are oriented preferentially in a ENE-WSW direction and slightly dip prograding towards the SSE, like Unit B's lenticular bodies (Figs. 3, 7 and 8).

CONCLUSIONS

The 3D models of the area studied are adequate for predicting the sedimentary heterogeneity that significantly influences fluid flow. Sedimentary heterogeneity is associated with the presence of the foreshore bars recognized in Unit B as gravelly, coarse- and medium-grained sandy lenticular bodies, which are interstratified and arranged in a specific direction, within a medium-grained sandy background.

Correlation between sedimentary facies and physical properties (i.e. grain size, porosity and permeability) enable models based on the distribution of a quantitative and continuous variable to be built (not of a qualitative and categorical one, like facies), which are suitable for flow simulation.

By applying the sequential conditional indicator simulation method, 3D models of reservoir not only satisfactorily reproduce the significant sedimentary heterogeneities generated by lenticular bodies, but also accurately predict and explain the spatial relationships and the 3D geometry of the sedimentary bodies that generate heterogeneity, using as input data outcrop interpretations (2D) of facies geometry. Nevertheless, the quality of models should be ensured by an accurate and consistent prior analysis of the spatial structure of the variable performed.

ACKNOWLEDGEMENTS

This study was carried out at the Geomodels Institute, which is sponsored by the Departaments d'Universitats, Recerca i Societat de la Informació (DURSI) of the Generalitat de Catalunya and the Instituto Geológico y Minero de España (IGME), and which includes the 3D Geological Modelling CER (University of Barcelona). Financial support was provided by Spain's Ministry of Education and Science (Projects CARES DGICYT BTE 2001-3650 and MARES CGL 2004-05816-C02-02) and the Generalitat de Catalunya (Grup Consolidat de Recerca de Geodinàmica i Anàlisi de Conques 2005SGR-00397). Research by P. Cabello was funded by a pre-doctoral grant from the DURSI and the European Fund. Grain size was determined at the Sedimentology Laboratory of the Departament d'Estratigrafia, Paleontologia i Geociències Marines (UB). Permeability and porosity were measured at the Geotechnical Laboratory of the Department of Geotechnical Engineering and Geosciences (UPC). The research benefited from collaboration with E. Abarca. We also acknowledge the valuable comments of Drs. E. Vàzquez-Suñé, A. Calafat, M. López-Blanco and by an anonymous reviewer, which all helped to improve the manuscript.

REFERENCES

Ainsworth, R.B., 2005. Sequence stratigraphic-based analysis of reservoir connectivity: influence of depositional architecture - a case study from marginal marine depositional setting. Petroleum Geoscience, 11, 257-276.

Arche, A., 1992. Deltas. In: Arche, A. (ed.). Sedimentología. Madrid, ed. Consejo Superior de Investigaciones Científicas, Vol I, 395-449.

Bhattacharya, J.P., Walker, R.G., 1992. Deltas. In: Walker, R.G., James, N.P. (eds.). Facies Models response to sea level change. Toronto, ed. Geological Association of Canada, 157-177.

Bitzer, K., 2004. Estimating paleogeographic, hydrological and climatic conditions in the upper Burdigalian Vallès-Penedès basin (Catalunya, Spain). Geologica Acta, 2(4), 321-331.

Cabello, P., López-Blanco, M., Falivene, O., Arbués, P., Ramos, E., Cabrera, Ll., Marzo, M., 2006. Modelos 3D de análogos de reservorios sedimentarios: Aplicación al sistema de abanico costero eoceno de Sant Llorenç del Munt (Cuenca del Ebro). Geotemas, 9, 45-48.

Castellini, A., Chawathé, A., Larue, D., Landa, J.L., Jian, F. X., Toldi, J.L., Chien, M. C., 2003. What is relevant to Flow? A Comprehensive Study Using a Shallow Marine Reservoir. SPE Reservoir Simulation Symposium, Houston, Texas. SPE eLibrary paper number 79669-MS.

Chilès, J-P., Delfiner, P., 1999. Geostatistics. Wiley series in probability and statistics. New York, ed. John Wiley & Sons, Inc., 695 pp.

Davis, J.C., 1986. Statistics and Data Analysis in Geology. New York, ed. John Wiley & Sons, Inc., 646 pp.

de Marsily, G., Delay, F., Teles, V., 1998. Some current methods to represent the heterogeneity of natural media in hydrogeology. Hydrogeology Journal, 6, 115-130.

Deutsch, C.V., 1999. Reservoir modelling with publicly available software. Computers & Geosciences, 25, 355-363.

Deutsch, C.V., Journel, A.G., 1992. Geostatistical Software Library and User's Guide. New York, ed. Oxford University Press, 340 pp.

Dreyer, T., Fält, L.M., Høy, T., Knarud, R., Steel, R., Cuevas, J.L., 1993. Sedimentary architecture of field analogues for reservoir information (SAFARI): a case study of the fluvial Escanilla Formation, Spanish Pyrenees. In: Flint, S., Bryant, I.D. (eds.). The Geological Modelling of Hydrocarbon Reservoirs and Outcrop Analogues. IAS Special Publication, 15, 57-80.

Falivene, O., Arbués, P., Gardiner, A., Pickup, G., Muñoz, J.A., Cabrera, Ll., 2006a. Best practice stochastic facies modelling from a channel-fill turbidite sandstone analog (the Quarry outcrop, Eocene Ainsa basin, northeast Spain). AAPG Bulletin, 90(7), 1003-1029.

Falivene, O., Arbués, P., Howell, J., Muñoz, J.A., Fernández, O., Marzo, M., 2006b. Hierarchical geocellular facies modelling of a turbidite reservoir analogue from the Eocene of the Ainsa basin, NE Spain. Marine and Petroleum Geology, 23, 679-701.

Falivene, O., Cabrera, Ll., Muñoz, J.A., Arbués, P., Fernández, O., Sáez, A., 2007a. Statistical grid-based facies reconstruction and modelling of sedimentary bodies. Alluvial-palustrine and turbiditic selected examples. Geologica Acta, 5(3), 199-230.

Falivene, O., Cabrera, Ll., Sáez, A., (2007b). Optimum and robust 3D facies interpolation strategies in a heterogeneous coal zone (Tertiary As Pontes basin, NW Spain). International Journal of Coal Geology. 71(2-3), 185-208.

Falivene, O., Cabrera, Ll., Sáez, A., (in press). Large to intermediate-scale aquifer heterogeneity in fine-grain dominated alluvial fans (Cenozoic As Pontes basin, NW Spain): Insight based on 3D geostatistical reconstruction. Hydrogeology Journal.

Gámez, D., Simó, J.A., Vàzquez-Suñé, E., Salvany, J.M., Carrera, J., 2005. Variación de las tasas de sedimentación en el Complejo Detrítico Superior del Delta del Llobregat (Barcelona): su relación con causas eustáticas, climáticas y antrópicas. Geogaceta, 38, 175-178.

Gómez-Hernández, J.J., Srivastava, R.M., 1990. ISIM3D: An ANSI-C three-dimensional multiple indicator conditional simulation program. Computers & Geosciences, 16(4), 395-440.

Gonçalvès, J., Violette, S., Robin, C., Bruel, D., Guillocheau, F., Ledoux, E., 2004. Combining a compaction model with a facies model to reproduce permeability fields at the regional scale. Physics and Chemistry of the Earth, 29, 17-24.

Gringarten, E., Deutsch, C.V., 2001. Variogram Interpretation and Modeling. Mathematical Geology, 33(4), 507-534.

Huggenberger, P., Aigner, T., 1999. Introduction to special issue on aquifer-sedimentology: problems, perspectives and modern approaches. Sedimentary Geology, 129, 179-186.

Jian, F.X., Larue, D.K., Castellini, A., Toldi, J., 2002. Reservoir Modeling Methods And Characterization Parameters For A Shoreface Reservoir: What Is Important For Fluid Flow Performance?. SPE Annual Technical Conference and Exhibition, San Antonio, Texas. SPE eLibrary Paper Number 77428-MS.

Journel, A.G., Alabert, F., 1989. Non-Gaussian data expansion in the Earth Sciences. Terra Nova, 1, 123-134.

Lafuerza, S., Canals, M., Casamor, J.L., Devincenzi, J.M., 2005. Characterization of deltaic sediment bodies based on in situ CPT/CPTU profiles: A case study on the Llobregat delta plain, Barcelona, Spain. Marine Geology, 222-223, 497-510.

Larue, D., 2004. Outcrop and waterflood simulation modeling of the 100-Foot Channel Complex, Texas and the Ainsa II Channel Complex, Spain: Analogs to multistory and multilateral channelized slope reservoirs. In: Gramer, M., Harris, P.M., Eberli, G.P. (eds.). Integration of outcrop and modern analogs in reservoir modeling: AAPG Memoir, 80, 337-364.

Larue, D., Legarre, H., 2004. Flow units, connectivity, and reservoir characterization in a wave-dominated deltaic reservoir: Meren reservoir, Nigeria. AAPG Bulletin, 88(3), 303-324.

Li, H., White, C.D., 2003. Geostatistical models for shales in distributary channel point bars (Ferron Sandstone, Utah): from ground-penetrating radar data to three-dimensional flow modeling. AAPG Bulletin, 87(12), 1851-1868.

MacDonald, A.C., Høye, T.H., Lowry, P., Jacobsen, T., Aasen, J.O., Grindheim, A.O., 1992. Stochastic flow unit modelling of a North-Sea coastal-deltaic reservoir. First Break, 10(4), 124-133.

Manzano, M., 1986. Estudio sedimentológico del prodelta Holoceno del Llobregat. Doctoral thesis. Universitat de Barcelona, 150 pp.

Manzano, M., Pelaez, M.D., Serra, J., 1986-87. Sedimentos prodeltaicos en el Delta emergido del Llobregat. Acta Geologica Hispanica, 21-22, 205-211.

Marqués, M.A., 1974. Las Formaciones Cuaternarias del Delta del Llobregat. Doctoral thesis. Universitat de Barcelona, 401 pp.

Marqués, M.A., 1984. Les Formacions Quaternàries del Delta del Llobregat. Barcelona, ed. Institut d'Estudis Catalans, 295 pp.

Reading, H.G., Collinson, J., 1996. Clastic coasts. In: Reading, H.G. (ed.). Sedimentary environments: Processes, Facies and Stratigraphy, 3th edition. Oxford, ed. Blackwell Science, 154-231.

Ricci Lucchi, F., 1978. Sedimentologia. Parte III. Ambiente Sedimentari e Facies. Bologna, ed. CLUEB, 504 pp.

Saaltink, M.W., Batlle, F., Ayora, C., Carrera, J., Olivella, S., 2004. RETRASO, a code for modeling reactive transport in saturated and unsaturated porous media. Geologica Acta, 2(3), 235-251.

Satur, N., Kelling, G., Cronin, B.T., Hurst, A., Gürbüz, K., 2005. Sedimentary architecture of a canyon-style fairway feeding a deep-water clastic system, the Miocene Cingöz Formation, southern Turkey: significance for reservoir characterisation and modelling. Sedimentary Geology, 173, 91-119.

Svanes, T., Martinius, A.W., Hegre, J., Maret, J.-P., Mjrs, R., Molina, J.C.U., 2004. Integration of subsurface applications to develop a dynamic stochastic modelling workflow. AAPG Bulletin, 88(10), 1369-1390.

Yaramanci, U., 2004. New technologies in groundwater exploration. Surface Nuclear Magnetic Resonance. Geologica Acta, 2(2), 109-120.

Zabalza-Mezghani, I., Manceau, E., Feraille, M., Jourdan, A., 2004. Uncertainty management: From geological scenarios to production scheme optimization. Journal of Petroleum Science and Engineering, 44, 11-25.

Zappa, G., Bersezio, R., Felletti, F., Giudici, M., 2006. Modeling heterogeneity of gravel-sand, braided stream, alluvial aquifers at the facies scale. Journal of Hydrology, 325, 134-153.

Manuscript received July 2006;
revision accepted March 2007.